2022

Seasonal controls on nearshore dissolved oxygen variability and hypoxia in a coastal embayment

Ryan K. Walter

Stephen A. Huie

(...)

Piero L.F. Mazzini

Ian Robbins

Estuarine, Coastal and Shelf Science 278 (2022) 108123

Contents lists available at ScienceDirect

Estuarine, Coastal and Shelf Science

journal homepage: www.elsevier.com/locate/ecss

Seasonal controls on nearshore dissolved oxygen variability and hypoxia in a coastal embayment

Ryan K. Walter [a,*], Stephen A. Huie [a], Jon Christian P. Abraham [a], Alexis Pasulka [b], Kristen A. Davis [c,d], Thomas P. Connolly [e], Piero L.F. Mazzini [f], Ian Robbins [a]

[a] Physics Department, California Polytechnic State University, San Luis Obispo, CA, USA
[b] Biological Sciences Department, California Polytechnic State University, San Luis Obispo, CA, USA
[c] Department of Civil and Environmental Engineering, University of California, Irvine, CA, USA
[d] Department of Earth System Science, University of California, Irvine, CA, USA
[e] Moss Landing Marine Laboratories, Moss Landing, CA, USA
[f] Virginia Institute of Marine Science, William and Mary, Gloucester Point, VA, USA

ARTICLE INFO

Keywords:
Dissolved oxygen
Hypoxia
Coastal upwelling
Upwelling shadow
Embayment

ABSTRACT

Declining dissolved oxygen (DO) is emerging as an increasingly important stressor in nearshore ecosystems, and there is a growing need to better understand DO dynamics and hypoxia risk in this highly variable environment. In this study, we collected data from monthly cruises on the inner shelf, continuous nearshore moorings inside and outside a small coastal upwelling embayment (San Luis Obispo Bay in Central California), and weekly phytoplankton measurements inside the bay during the upwelling season. Nearshore DO was generally dominated by low-frequency synoptic variability, with increased DO variance near the surface relative to the bottom and inside the bay compared to outside. Two nearshore hypoxic regimes were identified. In the first regime, which occurred during periods of strong upwelling in the spring across all nearshore sites, the nearshore bottom water temperature-DO (T-DO) relationship was aligned with that found offshore, suggesting hypoxia was driven by the direct advection and cross-shelf exchange of low DO subthermocline waters from the shelf. This period also coincided with minimal water-column stratification, small vertical DO differences, and a diatom-dominated phytoplankton assemblage. In the second regime, which occurred during summer months and was characterized by weaker upwelling, strong stratification, and dinoflagellate-dominated phytoplankton assemblage, the near-bottom T-DO relationship inside the bay deviated significantly from that on the shelf offshore. These hypoxic events inside the bay were likely driven by localized respiration and lack of ventilation of bottom waters due to strong stratification. Collectively, these observations reveal a shift in the strength and magnitude of physical versus biological processes driving nearshore DO dynamics. The high spatiotemporal variability of DO dynamics in upwelling bays means that they are likely to be at the forefront of ecosystem impacts of and adaptions to climate change, and may act as sentinel systems or "canaries on the coast."

1. Introduction

Declining dissolved oxygen (DO) levels continue to pose a major threat to marine ecosystems worldwide (Breitburg et al., 2018). Coastal regions are particularly susceptible to deoxygenation, and in recent decades, there has been an increased frequency and duration of hypoxic events in nearshore ecosystems, leading to direct mortality of and other significant non-lethal effects on economically and ecologically important fish and invertebrates (Grantham et al., 2004; Chan et al., 2008; Ekau et al., 2010; Gilbert et al., 2010; Booth et al., 2014). Furthermore, climate change is expected to exacerbate ocean deoxygenation and the prevalence of hypoxic events through ocean warming and further expansion of oxygen minimum zones (Keeling et al., 2010; Breitburg et al., 2018). Therefore, a better understanding of the processes that govern the spatial and temporal variability of nearshore DO and hypoxia risk is needed.

In Eastern Boundary Upwelling Systems (EBUS), like the California Current, seasonal variability in DO and the greatest risk for hypoxia occurs during the upwelling season (Siedlecki et al., 2015). During the so-called spring transition, strong upwelling favorable winds develop,

* Corresponding author.
E-mail address: rkwalter@calpoly.edu (R.K. Walter).

https://doi.org/10.1016/j.ecss.2022.108123
Received 23 February 2022; Received in revised form 14 October 2022; Accepted 16 October 2022
Available online 20 October 2022

leading to the cross-shelf advection of cold, oxygen-poor and nutrient-rich waters (Chavez and Messié, 2009; Checkley and Barth, 2009). This strong upwelling, coupled with local transport processes, can result in the net shoreward transport of DO-depleted waters onto the continental shelf (Grantham et al., 2004; Adams et al., 2013). Furthermore, the onshore flux of nutrients via upwelling fuels coastal productivity and subsequent microbial respiration over the shelf. Local respiration and other biogeochemical processes in both the water-column and benthic region can lead to further depletion of DO, highlighting the importance of both physical and biological processes for DO variability on the shelf (Connolly et al., 2010; Adams et al., 2013; Booth et al., 2014; Siedlecki et al., 2015). While major advances have been made in understanding drivers of DO variability in offshore shelf regions, there is still a need for an improved mechanistic understanding of DO dynamics in shallow nearshore habitats.

The shallow nearshore region is a dynamically complex environment. This is due to influence from both larger-scale shelf processes including changing wind-driven upwelling and offshore stratification (Walter et al., 2014a), as well as finer-scale nearshore processes such as internal waves and bores and the associated vertical mixing (Walter et al., 2012, 2014b; Sinnett et al., 2018; McSweeney et al., 2020); wave-, wind-, and tidal-driven flows (Woodson et al., 2007; Lentz and Fewings, 2011; Woodson, 2013; Walter et al., 2017); and buoyant plumes and fronts (Horner-Devine et al., 2015). Moreover, the presence of variable coastline orientation and topography (i.e., embayments, headlands, rocky reefs and kelp forests, etc.), as well as the presence of a coastal boundary layer, leads to complex nearshore circulation and retention patterns (Nickols et al., 2012; Largier, 2020; Trautman and Walter, 2021). This complex mosaic of transport processes and physical structure can drive significant local- and small-scale (on the order of km) DO variability and patchiness, leading to both increased risks for hypoxia exposure, as well as local refugia for nearshore organisms (Booth et al., 2012; Frieder et al., 2012; Pitcher et al., 2014; Walter et al., 2014a; Leary et al., 2017; Kapsenberg and Cyronak, 2019; Low et al., 2021). The nearshore physical environment also influences the impact that biological processes have on DO dynamics. Strong stratification can limit vertical mixing and isolate bottom waters from more aerated surface waters in contact with the atmosphere, thereby enhancing the impact of respiration on near-bottom DO. This impact is amplified in locally retentive systems such as coastal embayments, where there is a propensity for high biomass (e.g., dinoflagellate blooms) coupled with strong stratification (Bailey, 1991; Ryan et al., 2008; Pitcher and Probyn, 2011; Pitcher et al., 2014; Barth et al., 2020). Moreover, coastal eutrophication can also lead to oxygen loss in some nearshore upwelling systems with local anthropogenically enhanced nutrient loads, particularly in shallow and semi-enclosed bodies of water (Kessouri et al., 2021). A better understanding of seasonal controls on nearshore DO dynamics in different nearshore systems is needed in order to better predict and manage the onset, intensification, and ecosystem implications of low DO hypoxic events. Specifically, there is a need to further assess the role of retentive coastal embayments, which are found globally in EBUS and often termed upwelling bays (see recent review by Largier, 2020), in modulating the relative magnitude of local physical and biological processes that shape nearshore DO dynamics and the potential for highly localized microclimates.

In this study, we assessed nearshore DO variability and hypoxia risk inside and outside of a small upwelling bay (San Luis Obispo Bay) located along an understudied stretch of the Central California Coast. To better understand seasonal controls on DO variability, we deployed three nearshore moorings measuring both near-bottom and near-surface temperature and DO over the full upwelling season, capturing a range of environmental conditions spanning strong upwelling in the spring and the transition to weak upwelling during the late summer and early fall. We also collected offshore data from monthly cross-shelf transects to examine the extent to which nearshore DO variability reflected offshore patterns. Taking advantage of a co-located long-term harmful algal bloom (HAB) monitoring site, we investigated the role of phytoplankton community composition on DO variability inside the bay to help elucidate the role of physical and biological controls on seasonal DO dynamics. Collectively, these datasets reveal a clear seasonal shift in the magnitude of physical versus biological processes driving nearshore DO dynamics.

2. Experimental setup and methods

2.1. Site description

San Luis Obispo (SLO) Bay is a small (length and width scales less than 20 km, cf. Largier, 2020) and shallow (depths less than ~20 m inside bay), semi-enclosed coastal embayment located along an understudied stretch of the Central California Coast (Fig. 1). It is located ~200 km south of the well-characterized Monterey Bay and ~80 km north of Point Conception, a major marine biogeographic boundary, and the Santa Barbara Channel. To our knowledge, this is the first study to investigate nearshore DO dynamics in this stretch of the Central California coast (see also Valera et al., 2020 that utilized the data presented here in a machine learning modeling exercise). SLO Bay is home to a commercial fishing port, giant kelp forests that support high biodiversity and the endangered southern sea otter, and the California Polytechnic (Cal Poly) State University pier in the northern part of the bay (Fig. 1b). SLO Bay is also adjacent to several local marine protected areas (MPAs) including Pt. Buchon to the north. Additionally, the California Department of Fish and Wildlife (CDFW) fishing block that encompasses SLO Bay features substantial landings of market squid, Dungeness crab, groundfish, and salmon fisheries groups (Wang et al., 2022). The northern portion of SLO Bay is located downstream of a headland, and topographic shielding from regional northwesterly upwelling favorable winds leads to the seasonal formation of an upwelling shadow system (Walter et al., 2018) and convergent front (Trautman and Walter, 2021). Characterized at times by relatively warm and stratified waters, which are distinct from colder waters outside the bay, and high retention times, the upwelling shadow system is prone to harmful algal blooms (HABs) and hypoxic events that occasionally require shutting off the intake pipe into aquaria at the Cal Poly Pier (Walter et al., 2018; Barth et al., 2020).

2.2. Data

To characterize nearshore DO variability inside and outside the bay, three oceanographic moorings were deployed along the 18 m isobath over the upwelling season from March to late August 2017 (Fig. 1b). One mooring was located in the middle of the embayment (Middle Bay – MB), one inside the bay on the southern end (South Bay – SB), and one outside the bay to the north (North Bay – NB) (Fig. 1b). Each mooring was equipped with near-bottom [2 m above bed (mab)] and near-surface (15 mab) instruments measuring temperature and DO. The bottom instruments were Sea-Bird Scientific 37 SMP-ODO conductivity-temperature-depth (CTD) sensors with an in-line (i.e., pumped through the anti-biofouling devices) optical DO sensor (SBE 63), sampling every 10 min. Surface measurements (1 min sampling period) were made with Precision Measurement Engineering miniDOT sensors, equipped with copper mesh and plates for anti-biofouling. All DO sensors were calibrated by the respective manufacturer prior to deployment, and sensors were checked and cleaned by divers approximately monthly for optimal performance. Several sensors stopped recording early due to instrument error and/or battery issues (e.g., NB15 in early July; see Fig. 1). To examine the relationship between offshore shelf waters and nearshore DO variability, a series of monthly cross-shelf transects from the 30 m isobath out to the 300 m isobath were also performed onboard Cal Poly's R/V Richards (Fig. 1). During each of the offshore transects, vertical profiles of temperature and DO were measured at the 30, 50, 100, 150, 200, and 300 m isobaths using a Sea-Bird Scientific 19+ profiling CTD equipped with an electrochemical DO sensor (SBE 43, calibrated by

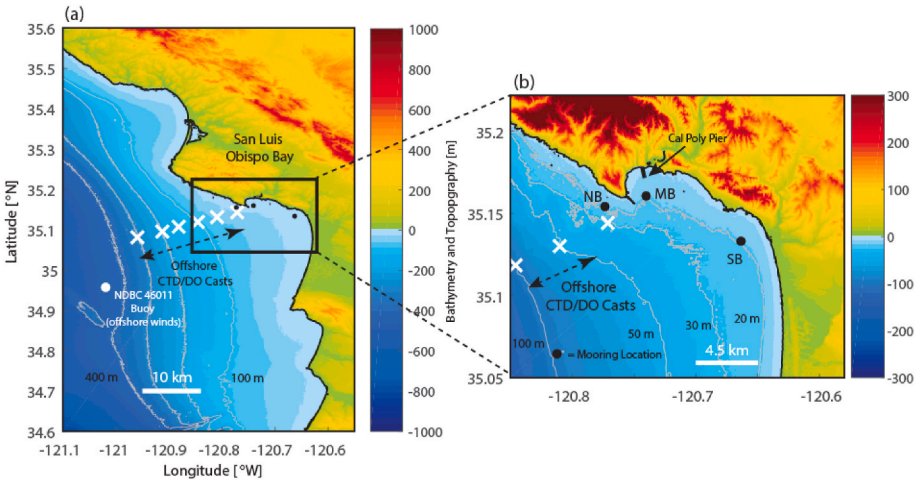

Fig. 1. Topography and bathymetry of the SLO Bay study region in Central California. (a) Zoomed out view of the region highlighting the locations of the offshore CTD/DO casts (white 'X') and the regional buoy used to measure upwelling winds. (b) Zoomed in view of San Luis Obispo Bay highlighting mooring locations (black dots) in the North Bay (NB), Middle Bay (MB), and South Bay (SB), as well as the location of the Cal Poly Pier (thick black line with label).

manufacturer prior to study). These transects were completed on 3 March, 17 April, 22 May, 23 June, 11 July, and 8 August 2017.

To help elucidate potential biological controls on nearshore DO variability, we utilized data from several long-term monitoring programs at the Cal Poly Pier, located inside the bay near MB (Fig. 1). The first data source was weekly surface phytoplankton abundance and community composition data collected as part of the California HAB Monitoring and Alert Program (see detailed description in Barth et al., 2020; https://erddap.sccoos.org/erddap/tabledap/HABs-CalPoly.html). The second data source was from an automated profiling water quality package that takes vertical profiles of temperature, conductivity (salinity), and chlorophyll fluorescence approximately every 30 min (see detailed description in Walter et al., 2018; https://erddap.cencoos.org/erddap/info/san-luis-bay-cal-poly-pier-shore/index.html). The weekly surface HAB measurements provided data on phytoplankton community composition, while the near continuous profiler measurements quantified changes in abundance with depth inside the bay. Following Barth et al. (2020), we used the ratio of total dinoflagellates to total diatoms to assess changes in community composition. To investigate the influence of regional wind-driven upwelling, offshore winds were obtained from the National Data Buoy Center (NDBC) buoy 46011 (Fig. 1; https://www.ndbc.noaa.gov/station_page.php?station=46011). Upwelling favorable winds were calculated as equatorward and parallel to the coastline (150° from true north, cf. Walter et al., 2018).

2.3. Data processing

Timescales of variability for temperature and DO were quantified using spectral analysis. Welch's method with Hamming windows and 50% overlap between adjacent segments was utilized to minimize spectral leakage, with window length selected by taking into account the length of the original record, frequency resolution, and the degrees of freedom (DOF) for confidence interval estimates, which were estimated using a chi-squared variable analysis and the equivalent DOF (Emery and Thomson, 2004). Spectra were then integrated across various frequency ranges representing low-frequency [0.07 to 0.75 cycles per day (cpd)], daily (0.75–1.25 cpd), daily to half-daily (1.25–1.75 cpd), half daily (1.75–2.25 cpd), hourly (2.25–24 cpd), and high-frequency [24 cpd to 3 cycles per hour (cph)] bands to quantify the relative variance in each band (e.g., Guadayol et al., 2014; Low et al., 2021). To assess seasonal controls on nearshore DO variability and the connection to offshore shelf waters, hourly averaged nearshore DO data were low-pass filtered (33 h) to remove higher-frequency variability possibly driven by tides, local diurnal wind forcing, fronts, and internal waves (cf. Walter et al., 2017). The role of high-frequency processes on nearshore DO variability, although relatively small (see e.g., Section 3.1.2), will be investigated in a future study.

To examine the extent to which offshore shelf waters were similar to nearshore waters, and by extension the role that nearshore processes play in modulating DO variability, we explored temperature-DO (T-DO) relationships for the offshore shelf data obtained from boat-based surveys and compared these to T-DO relationships from the moored nearshore data at all three sites (cf. Connolly et al., 2010). We also explored how the nearshore T-DO parameter space changed over time in response to variable upwelling wind forcing, vertical temperature stratification (difference between near-surface and near-bottom temperature at each respective site), vertical DO gradients (difference between near-surface and near-bottom DO at each respective site), and depth-integrated chlorophyll and phytoplankton community composition (ratio between dinoflagellates and diatoms) from the Cal Poly Pier. A k-means cluster analysis was also performed using the T-DO parameter space plot, and means and standard deviations of the aforementioned variables were calculated in each cluster to identify and describe different DO forcing regimes. A k-means clustering analysis partitions data into k clusters, minimizing the within-cluster variances to each respective cluster centroid (Lance and Williams, 1967). A silhouette analysis was performed to identify the optimal number of clusters ($k = 3$).

In what follows, we adopt a definition for hypoxic waters as below 4.6 mg/L following the broad comparative analysis of Vaquer-Sunyer and Duarte (2008) that identified this concentration as a critical biological threshold (e.g., lethal threshold for 10% of marine benthic communities studied). This definition captures low DO events that potentially adversely impact local ecosystems. For example, Mattiasen et al. (2020) found that their 4.1 mg/L "moderate hypoxia" treatment had a negative effect on kelp forest fish metabolism. We recognize that some species' limits, including both lethal and sublethal limits, will be different [e.g., 2 mg/L is also sometimes used as a hypoxic threshold, but Vaquer-Sunyer and Duarte (2008) found that this was below the empirical lethal and sublethal threshold for half of the species in their analysis] and that there are likely region- and site-specific differences among species. For example, Vaquer-Sunyer and Duarte (2008) analyzed many taxa not found in the nearshore of the California Current. Hofmann et al. (2011) summarized a range of thresholds used to identify hypoxia in the literature, with 2 mg/L ("coastal hypoxia") commonly used in coastal ecosystems where communities may be adapted to low oxygen conditions; however, there are limited studies of hypoxia threshold data available from nearshore California Current taxa. A review by Gray et al. (2002) found that the growth of organisms in the

water column is affected at concentrations between 4.5 and 6 mg/L and other aspects of metabolism were affected between 2 and 4 mg/L. Recognizing that there are species-dependent responses, we identify events below 4.6 mg/L (and also highlight the 2 mg/L threshold in most figures) as hypoxic events that could potentially adversely affect nearshore organisms. Regardless of the threshold utilized, this paper highlights mechanisms and processes that lead to low DO events over a range of hypoxic thresholds identified in the literature. We utilize mg/L as our unit of choice for DO concentrations based on historical precedence from a management and regulatory perspective. For reference, 4.6 mg/L (2.0 mg/L) is approximately equal to 3.22 ml/L (1.40 ml/L), 140.16 μmol/kg (60.94 μmol/kg), and 107.70 matm (46.82 matm) for seawater at atmospheric pressure with a temperature of 11.4 °C and a salinity of 33.7 (mean temperature and salinity values at MB2 during the experiment).

3. Results

3.1. Nearshore data

3.1.1. General observations

Upwelling favorable winds were strongest, but also highly variable (e.g., 1–2 week upwelling-relaxation cycles), during the spring and early summer (Fig. 2a). During the late summer, upwelling winds decreased in magnitude and were less variable. Nearshore surface and bottom temperatures at all sites progressively warmed from spring to summer, with vertical differences between surface and bottom waters (i.e., temperature stratification) increasing progressively in the summer (Fig. 2b and c). Near-surface waters generally displayed more temperature variance compared to near-bottom waters. Near-bottom temperatures were largely consistent across the three nearshore sites, while at the surface, the outside bay site (NB) was generally colder than the inside bay sites (MB and SB), particularly in the summer. DO also displayed less variance near the bottom, with concentrations consistently dropping below 4.6 mg/L during both the spring and summer at all sites and below 2 mg/L during the late summer inside the bay at MB and SB (Fig. 2d and e, and S1). Hypoxic conditions inside the bay (MB and SB) were present a greater percentage of the time with longer event durations, lower minimum DO concentrations, and shorter recurrence intervals on average compared to outside the bay at NB (see Fig. S1 and event statistics in Table S1). Similar to temperature, near-surface DO was consistently higher and more variable compared to near-bottom DO. Near-bottom DO inside the bay (MB and SB) was consistently lower than near-bottom DO outside the bay (NB) during the summer. Depth-integrated chlorophyll concentrations from the Cal Poly Pier inside the bay showed synoptic-scale (i.e., event-scale) variability throughout the experiment, with the largest events observed in the late spring (Fig. 2f). These events were linked with prolonged upwelling events and also coincided with increases in nearshore surface DO and decreases in bottom DO. The surface phytoplankton community composition inside

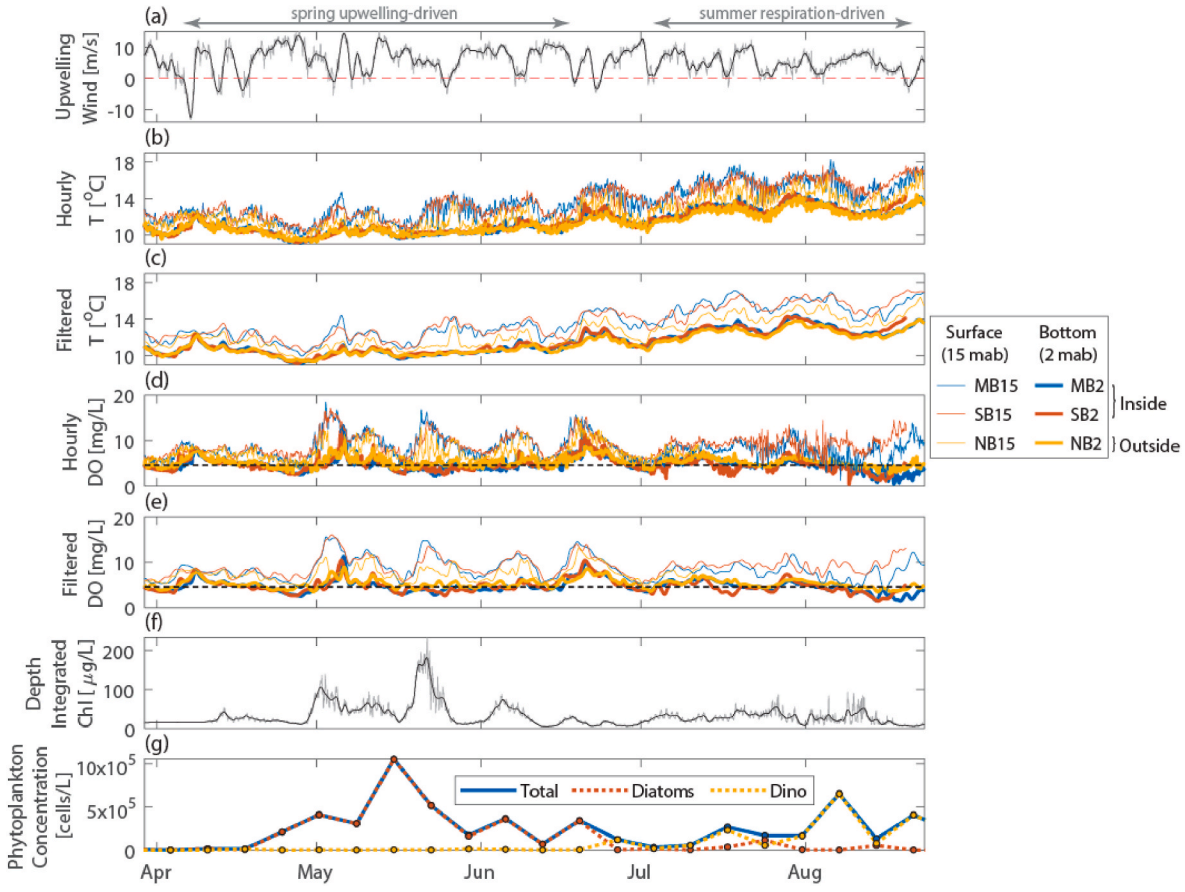

Fig. 2. Time series from late March to late August. (a) Upwelling favorable winds, with the hourly (gray) and low-pass filtered (black) data. (b) Hourly temperature, (c) low-pass filtered temperature, (d) hourly dissolved oxygen, and (e) low-pass filtered dissolved oxygen at each mooring (Outside Bay: NB – orange; Inside Bay: MB – blue and SB – red). The thick lines in the panels b–e correspond to the near-bottom (2 mab) measurements, while the thin lines denote the near-surface (15 mab). The dashed line in panels (d) and (e) represents the hypoxic threshold of 4.6 mg/L. (f) Depth-integrated chlorophyll measured from the Cal Poly Pier profiler inside the bay (gray) and the low-pass filtered quantity (black). (g) Surface phytoplankton concentration and community composition from inside the bay at the Cal Poly Pier. Nearshore sites MB and SB are inside the bay and NB is outside the bay (Fig. 1). The light gray arrows at the top denote the approximate timing of the two hypoxic regimes identified (Section 4.1). (For interpretation of the references to color in this figure legend, the reader is referred to the Web version of this article.)

the bay was dominated by diatoms in the spring and early summer, transitioning to dinoflagellate-dominated waters in the late summer (Fig. 2g).

3.1.2. Timescales of DO variability

Across all nearshore sites, near-surface DO variance was consistently higher compared to near-bottom DO (Fig. 3). Both near-bottom and near-surface DO variance displayed a slight increase in May and June

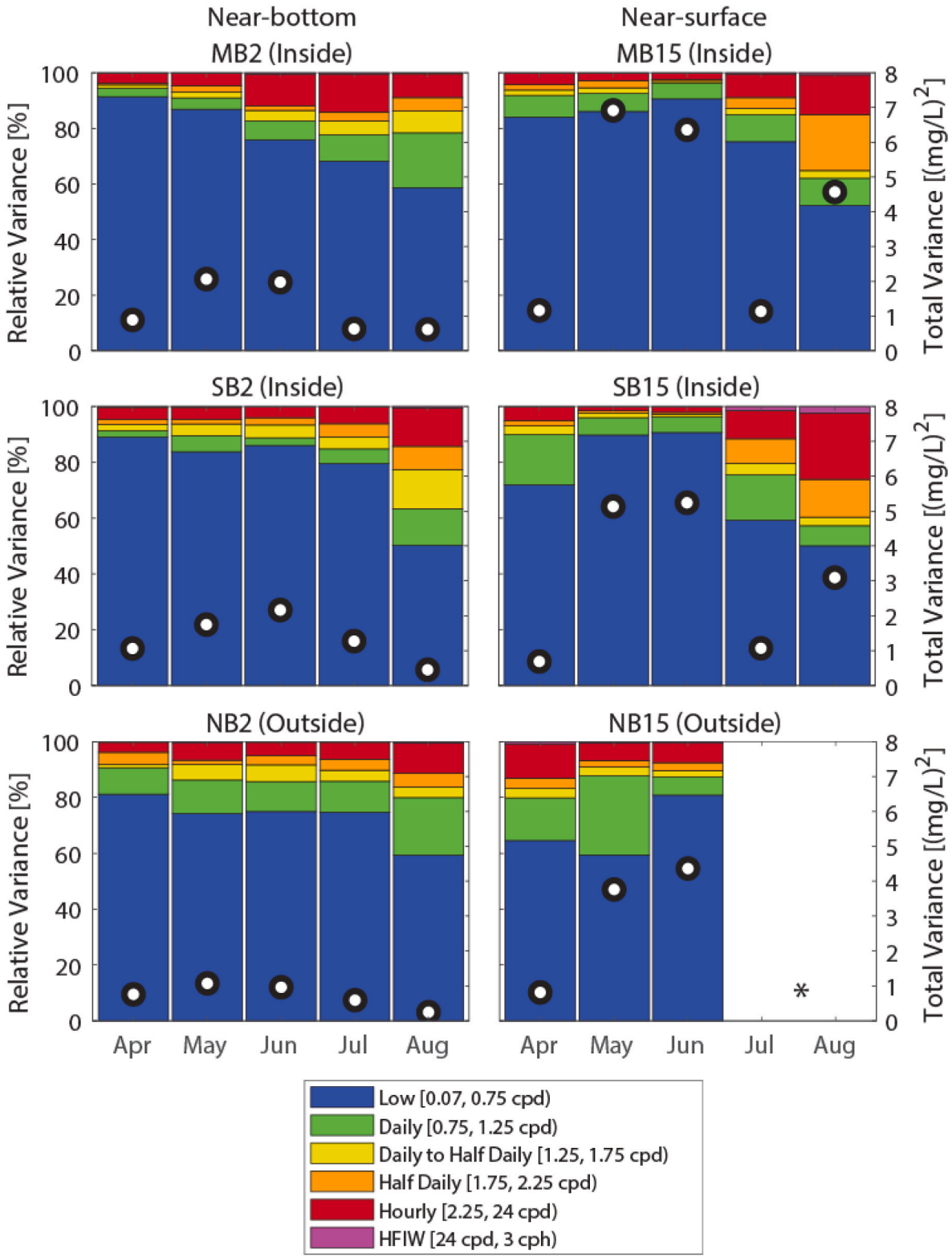

Fig. 3. Variance decomposition of near-bottom (left column) and near-surface (right column) DO at each nearshore site (rows) for each month during the experiment. The left axis represents the relative variance, calculated by integrating the respective monthly spectra in the frequency bins shown in the legend (see also Section 2.3) and dividing by the total variance (right axis; white circles) calculated by integrating the respective monthly spectra across all frequencies. *NB15 data are not available for July and August (see Section 2.2). Nearshore sites MB and SB are inside the bay and NB is outside the bay (Fig. 1).

compared to other months. DO variability across all sites was dominated by the low-frequency band (0.07–0.75 cpd) across all months. The contribution of higher frequency processes (i.e., frequencies larger than the low-frequency band limit of 0.75 cpd) to DO variability increased slightly in the summer months.

3.2. Offshore T-DO patterns

The T-DO parameter space for all sampling dates at the offshore shelf locations consistently showed a strong positive relationship between temperature and DO (Fig. 4). Additionally, the T-DO relationship in deep waters (low T-DO regions in Figs. 4 and 5) at the furthest offshore location (300 m) varied minimally over the study period with DO concentrations typically varying less than 1 mg/L for a given temperature. The high T-DO region of the parameter space was moderately variable across the sampling dates, but still displayed a consistent positive relationship between temperature and DO (Fig. 5).

3.3. Linking nearshore and offshore data

3.3.1. Near-bottom relationships

The near-bottom, nearshore data aligned with the offshore data in the low T-DO region of the parameter space across all three nearshore sites (Fig. 6). This is in contrast to the high T-DO region of the parameter space, where the nearshore DO data deviated significantly below the offshore DO data for a given temperature. This pattern was most pronounced for nearshore sites located inside the bay (MB and SB), with much smaller deviations outside the bay (NB). In general, the nearshore sites inside the bay (MB and SB) were marked by an increased number of hypoxic events and lower DO concentrations during these events relative to outside the bay (NB), especially during mid to late summer.

Closer examination of the low DO hypoxic events (e.g., below 4.6 mg/L) revealed two distinct regimes in the T-DO parameter space. In the low T-DO hypoxic regime, corresponding to when the nearshore and offshore T-DO relationships closely tracked one another in the spring months (Fig. 6a–c), upwelling winds were strongest (Fig. 6d–f), vertical temperature stratification was minimal (Fig. 6g–i), and there were minimal vertical DO differences (Fig. 6j-l). In the other nearshore hypoxic regime at higher temperatures, where the nearshore DO data was significantly lower than offshore DO data for a given temperature, upwelling was weak to moderate (Fig. 6d–f), vertical temperature

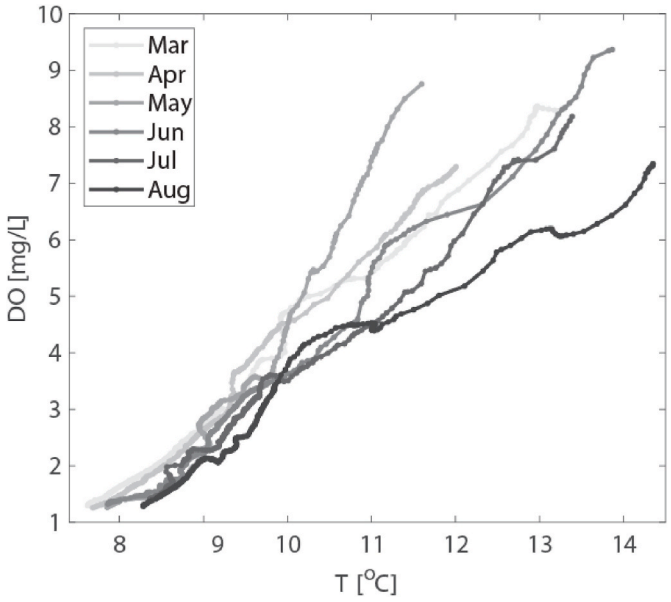

Fig. 5. Temperature-DO relationship for the 300 m profile location for all offshore cruises. Gray-scale colors denote the month of the cruise, with the earliest cruise (Mar) is shown in the lightest gray progressing to darker grays with the latest monthly cruise (Aug) in black.

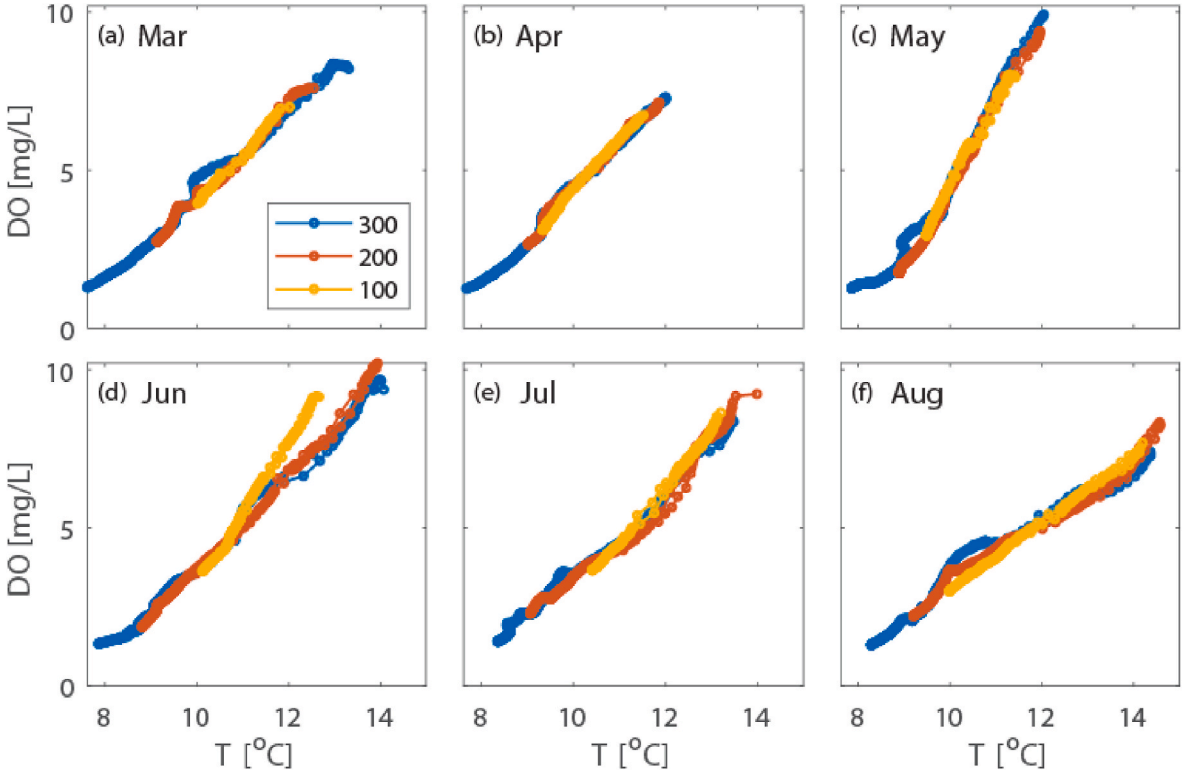

Fig. 4. Temperature-DO relationships for the 300 m (blue), 200 m (red), and 100 m (orange) profiles across all offshore cruises. (For interpretation of the references to color in this figure legend, the reader is referred to the Web version of this article.)

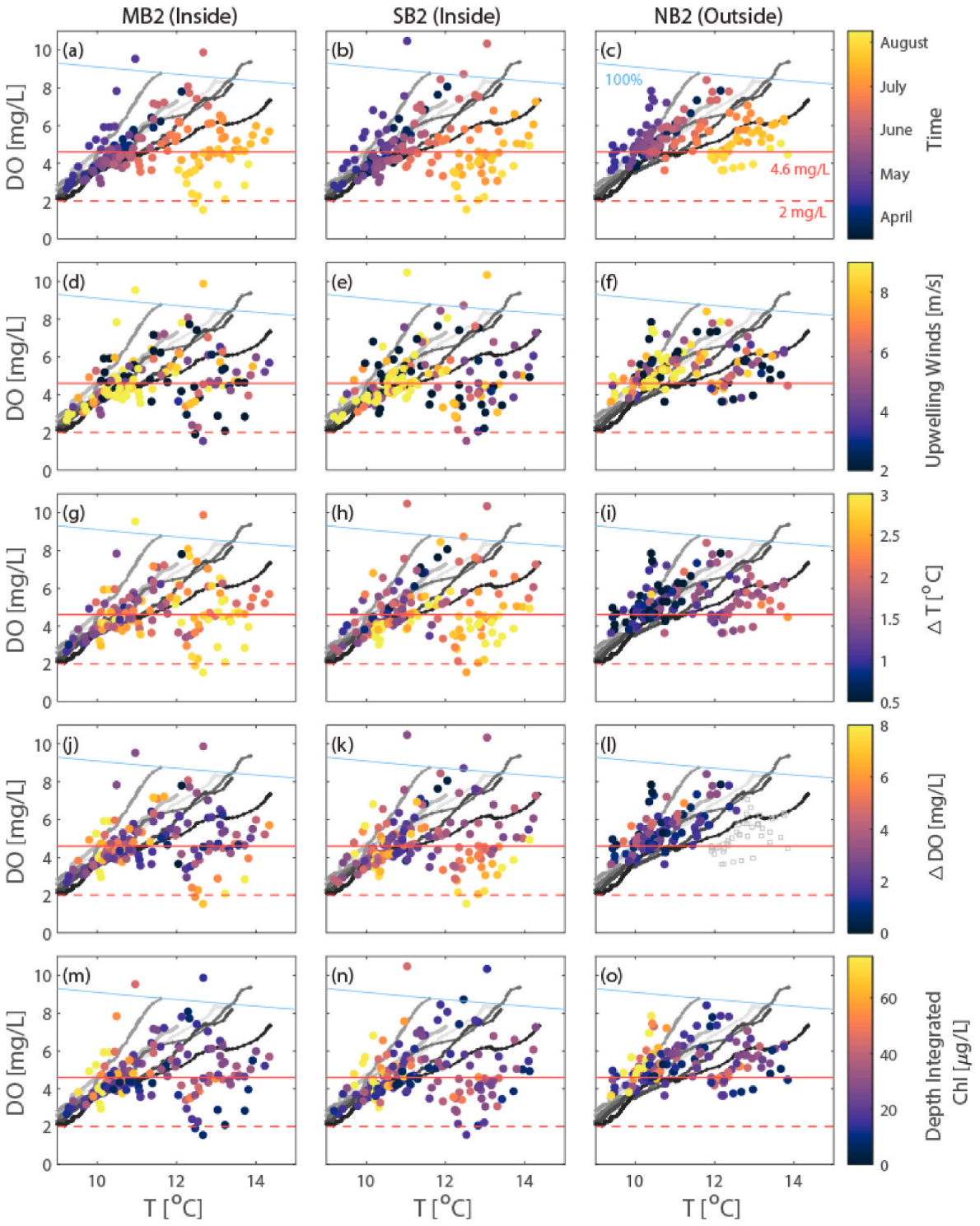

Fig. 6. Near-bottom (2 mab) temperature-DO relationship from MB (left column), SB (middle column), and NB (right column). Hourly data are low-pass filtered and then downsampled (one point every 24 h) for visualization. The colors on each plot represent the time (a–c), upwelling favorable winds (d–f), vertical temperature stratification at the respective sites (difference between near-surface and near-bottom temperature) (g–i), vertical DO gradients at the respective sites (difference between near-surface and near-bottom DO) (j–l), and depth-integrated chlorophyll at the Cal Poly Pier inside the bay (m–o). Also shown in each plot in small grayscale points are the offshore T-DO relationship from 300 m profile location, with the earliest monthly cruise (Mar) in the lightest gray and the latest monthly cruise (Aug) in black. Hypoxic thresholds of 2 and 4.6 mg/L are shown as a horizontal dashed and solid red line, respectively. The light blue line denotes 100% oxygen concentration at 1 atm and a mean salinity of 33.7. In panel (l), gray squares are shown when near-surface DO data were not available. Nearshore sites MB and SB are inside the bay and NB is outside the bay (Fig. 1). (For interpretation of the references to color in this figure legend, the reader is referred to the Web version of this article.)

stratification was strongest (Fig. 6g–i), and the largest vertical DO differences were observed (Fig. 6j-l). This regime occurred exclusively in the mid to late summer, and the patterns above were more pronounced inside the bay (MB and SB) compared to outside the bay (NB) where there were only minimal deviations from offshore T-DO patterns and vertical temperature stratification remained small (Fig. 6i). The two sites inside the bay (MB and SB) showed largely similar patterns and relationships.

There were minimal trends displayed between depth-integrated chlorophyll inside the bay (no chlorophyll data available outside the bay) and the offshore and nearshore T-DO relationship at all sites (Fig. 6m–o). The largest depth-integrated chlorophyll values inside the bay occurred in the low T-DO region of the parameter space (although not significantly below the hypoxic threshold of 4.6 mg/L), with moderate values in the higher temperature region.

3.3.2. *Near-surface relationships*

The near-surface nearshore data displayed significantly more

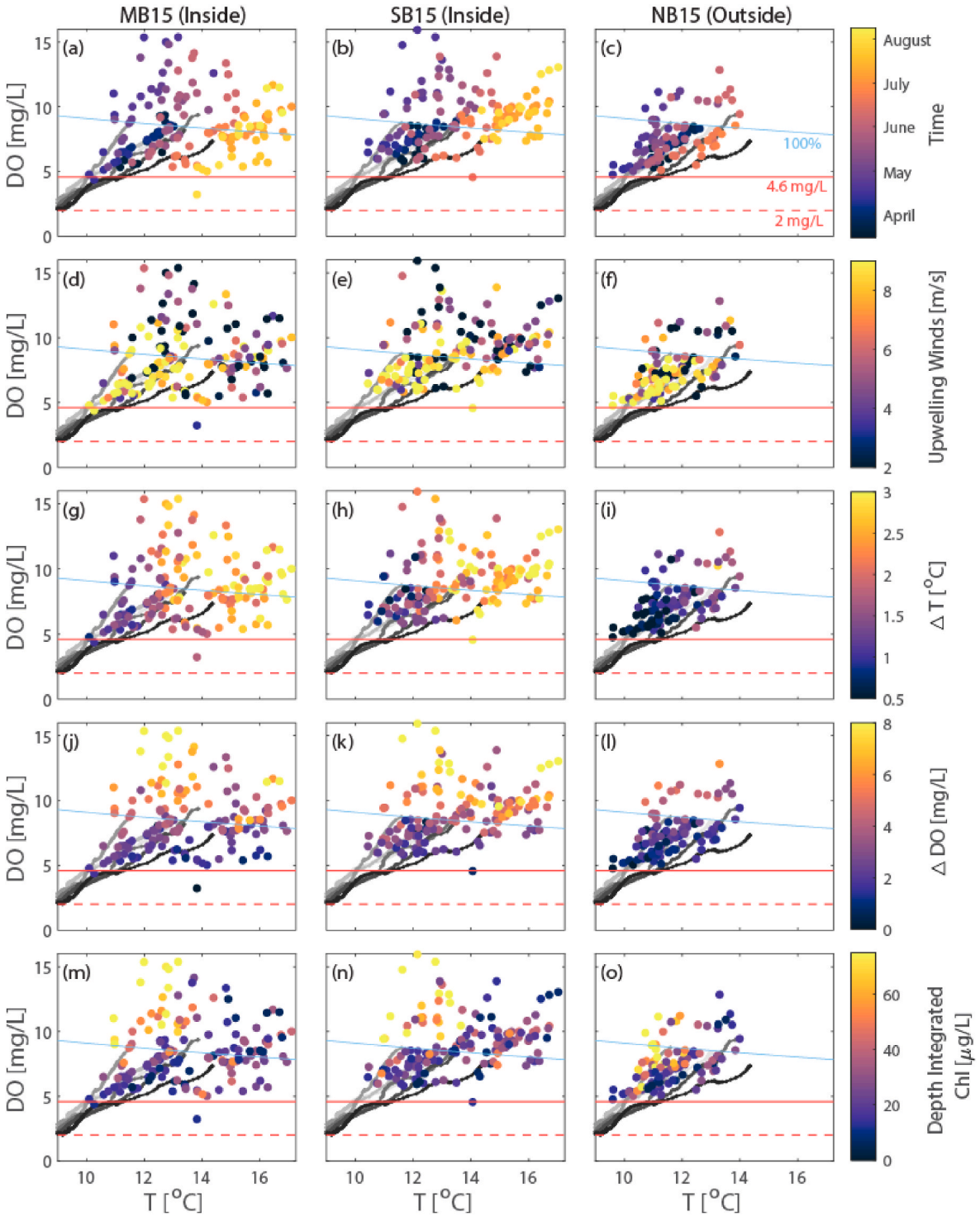

Fig. 7. Same as Fig. 6 except for near-surface (15 mab) measurements. NB15 data (third column) not available for part of July and August (see Section 2.2). Note the different x- and y-axis limits for Figs. 6 and 7.

variability in the T-DO parameter space (Fig. 7). As expected, DO concentrations were significantly higher compared to the near-bottom values, particularly inside the bay (MB and SB), with concentrations above the hypoxic threshold almost exclusively. The surface data inside the bay (MB and SB) generally tracked T-DO patterns outside the bay (NB), but the data from inside the bay (MB and SB) commonly showed larger DO concentrations for a given temperature compared to outside the bay (NB), particularly in the mid to high temperature range. The nearshore T-DO data largely followed the offshore T-DO trends, but also extended the parameter space into a higher T-DO region not measured on the shelf. During periods of strong upwelling in the spring months, the near-surface nearshore T-DO data aligned with the offshore T-DO data (Fig. 7a–f). The high T-DO region of the parameter space typically corresponded with the largest vertical stratification and vertical DO differences inside the bay (MB and SB), whereas outside the bay (NB) showed minimal vertical differences in temperature and DO (Fig. 7g–i). The largest DO values inside the bay (MB and SB) were observed when the depth-integrated chlorophyll inside the bay was also largest (Fig. 7j and k). Outside the bay (NB), where no chlorophyll data were available, DO concentrations were not as large during these bloom events measured inside the bay. Like the near-bottom data, the two sites inside the bay (MB and SB) showed largely similar patterns and relationships.

3.4. Phytoplankton community composition effects

Inside the bay (MB), there was a clear seasonal progression from diatom-dominated communities in the spring and early summer in the presence of colder waters transitioning to dinoflagellate-dominated communities in the mid to late summer with warmer waters (Fig. 8). For the near-bottom hypoxic regime previously identified (Section 3.3.1) when the nearshore T-DO aligned with the offshore data in the low T-DO region of the parameter space in the spring months with strong upwelling, diatom communities were present at the highest concentrations (Fig. 8d–f). For the other near-bottom hypoxic regime when the nearshore DO data deviated significantly below the offshore DO data at higher temperatures in the summer months, dinoflagellate communities were present at the highest concentrations.

4. Discussion

4.1. Seasonal variations in physical and biological processes contribute to distinct nearshore hypoxic regimes

4.1.1. Spring upwelling-driven nearshore hypoxic regime

Two nearshore hypoxic regimes were identified in the near-bottom mooring data when DO concentrations dropped below potentially deleterious levels (e.g., 4.6 mg/L). In the first regime, which occurred during the spring months, the nearshore T-DO data directly overlapped with the offshore shelf T-DO data in the low temperature and low DO region of the T-DO parameter space. This regime also emerged as one of the delineated clusters in the k-means cluster analysis (Fig. 9, "Cluster 1 Upwelling Driven"; Table 1). Given the direct correspondence to the offshore shelf waters and the concurrent strong upwelling, these low DO waters are likely the result of upwelling-driven cross-shelf exchange of low DO subthermocline waters. The advection of these waters into the nearshore led to minimal water-column stratification and phytoplankton communities dominated by diatoms, which thrive in unstratified, nutrient-rich waters (Anderson et al., 2008; Silva et al., 2009; Barth et al., 2020). This regime and cluster were consistent across the nearshore sites both inside the bay (MB and SB) and outside the bay (NB). Interestingly, the two nearshore sites inside the bay (MB and SB) showed slightly lower temperatures and DO concentrations in this regime compared to outside the bay (NB) (Figs. 6 and 9). Colder bottom waters inside of upwelling bays relative to those at comparable depths over adjacent open coastlines has been documented elsewhere, although the dynamics that control the spatial intensification of upwelling near headlands are still poorly understood and warrant further research (cf. Largier, 2020).

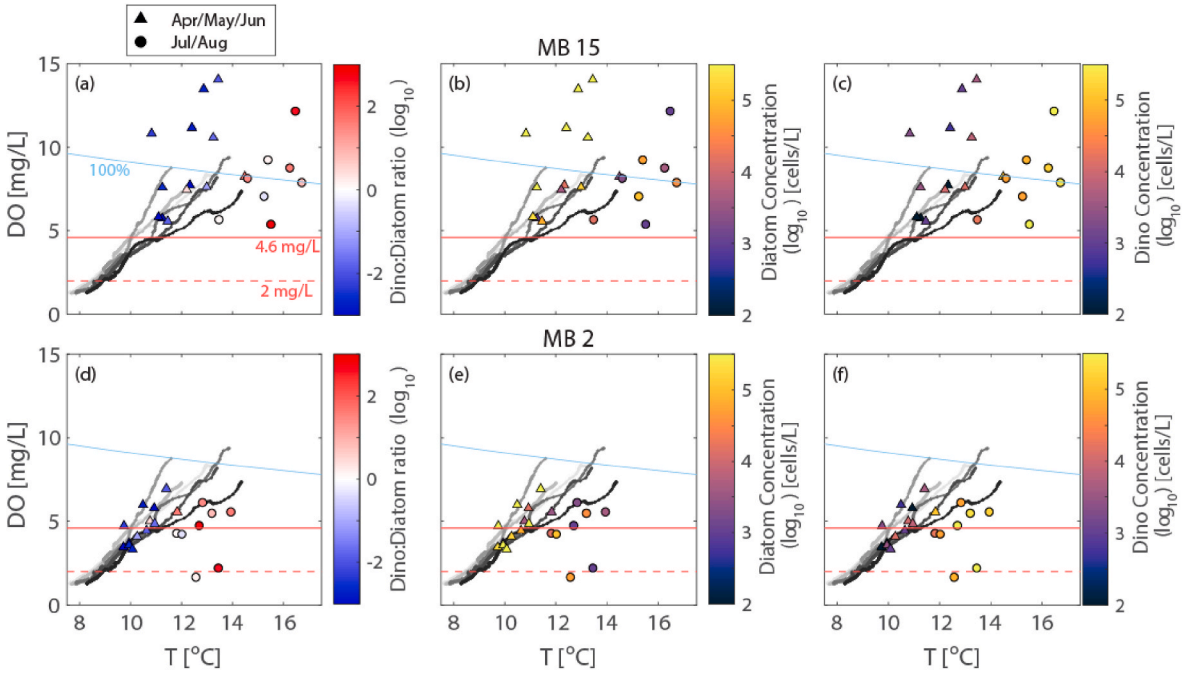

Fig. 8. Inside the bay (MB) surface (a–c) and bottom (d–f) T-DO relationships, as in Figs. 6 and 7, respectively. Plots (a) and (d) are colored by the $\log_{10}$ ratio of dinoflagellates to diatoms. Plots (b) and (e) are colored by the $\log_{10}$ diatom concentration. Plots (c) and (f) are colored by the $\log_{10}$ dinoflagellate concentration. Also shown in each plot in small grayscale points are the offshore T-DO relationship from 300 m, with the earliest cruise in the lightest gray and the latest cruise in black. Hypoxic thresholds of 2 and 4.6 mg/L are shown as a horizontal dashed and solid red line, respectively. The light blue line denotes 100% oxygen concentration at 1 atm and a mean salinity of 33.7. Colored triangles denote data from spring months (April, May, and June), while colored circles are from summer months (July and August). (For interpretation of the references to color in this figure legend, the reader is referred to the Web version of this article.)

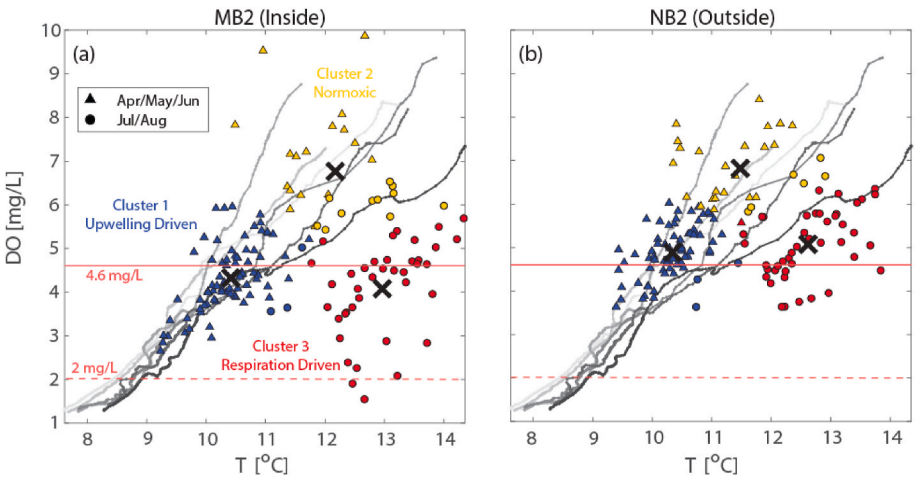

Fig. 9. K-means cluster analysis for the near-bottom (2 mab) T-DO relationships from (a) MB (inside the bay) and (b) NB (outside the bay), as in Fig. 6. The black 'X' denotes the centroid of each of the three labelled clusters. Colored triangles denote data from spring months (April, May, and June), while colored circles are from summer months (July and August). Also shown in each plot in small grayscale points are the offshore T-DO relationship from 300 m, with the earliest cruise in the lightest gray and the latest cruise in black. Hypoxic thresholds of 2 and 4.6 mg/L are shown as a horizontal dashed and solid red line, respectively. (For interpretation of the references to color in this figure legend, the reader is referred to the Web version of this article.)

Table 1
Mean and standard deviation for each of the different k-means clusters identified in Fig. 9 for near-bottom data inside the bay (MB) and outside the bay (NB). *Phytoplankton community composition data are calculated from weekly values (obtained from weekly samples inside the bay at the Cal Poly Pier). No phytoplankton community composition data are available outside the bay at the NB site and thus are designated "NA" in the table.

Site	Cluster	DO [mg/L]	T [°C]	Upwelling Winds [m/s]	△DO [mg/L]	△T [°C]	*Dino:Diatom Ratio [$\log_{10}$]
MB2 (Inside)	Upwelling Driven (1)	4.32 ± 0.77	10.42 ± 0.54	6.33 ± 4.23	4.02 ± 2.39	1.83 ± 0.63	−1.48 ± 1.28
	Normoxic (2)	6.76 ± 1.12	12.17 ± 0.78	5.12 ± 4.45	3.04 ± 1.53	2.19 ± 0.68	0.06 ± 1.80
	Respiration Driven (3)	4.08 ± 1.07	12.96 ± 0.66	4.49 ± 3.03	3.67 ± 2.16	2.60 ± 0.57	1.80 ± 1.05
NB2 (Outside)	Upwelling Driven (1)	4.89 ± 0.59	10.34 ± 0.44	6.43 ± 4.02	2.06 ± 1.2	0.91 ± 0.45	NA
	Normoxic (2)	6.82 ± 0.72	11.48 ± 0.74	4.78 ± 5.24	2.1 ± 1.63	1.14 ± 0.56	NA
	Respiration Driven (3)	5.08 ± 0.75	12.62 ± 0.64	4.82 ± 2.89	1.63 ± 0.2	1.62 ± 0.32	NA

In this regime, strong upwelling caused the cross-shelf advection of low DO subthermocline waters on the shelf into the nearshore. Moreover, the lack of stratification in the nearshore during this time likely led to enhanced vertical mixing of oxygen-rich surface waters (e.g., through air-sea gas exchange and/or production via photosynthesis) and possibly buffered against further biological drawdown via the degradation of organic matter following nearshore diatom blooms. In general, nearshore DO variability was governed by low-frequency processes (0.07–0.75 cpd, Fig. 3) and timescales of DO variability that typically matched synoptic variability in upwelling wind forcing (e.g., one to two week upwelling-relaxation cycle timescales). This was especially the case during the spring when synoptic-scale upwelling variability was strongest and upwelling relaxation events likely led to the greatest exchange of waters between the bay and the adjacent shelf and a "reset" of the retentive bay system (e.g., Walter et al., 2017; Trautman and Walter, 2021). This, coupled with the lack of strong stratification and enhanced vertical mixing, might be why high chlorophyll periods observed during the spring months did not drive significant local modulation and drawdown of bottom DO waters.

4.1.2. Summer stratification and respiration-driven nearshore hypoxic regime

The second nearshore hypoxic regime identified occurred during the summer months and at higher temperatures in the T-DO parameter space. This regime was much more pronounced inside the bay (MB and SB) compared to outside the bay (NB) where it was largely absent, with DO concentrations inside the bay consistently below 4.6 mg/L and at their lowest levels measured during the experiment at less than 2 mg/L. During the summer low DO event when concentrations dropped below 2 mg/L inside the bay, research aquaria at the Cal Poly Pier, which receive water from an intake pipe located at the southern end of the pier, had widespread fish kills of juvenile fish, including many that are endemic to local waters (e.g., *Sebastes* spp.; T. Moylan, personal communication). In this regime and cluster (Fig. 9, Cluster 3), nearshore DO values were considerably lower than offshore shelf concentrations for a given temperature and time, suggesting local nearshore modification and DO drawdown. Moreover, compared to the upwelling-driven hypoxic regime, this regime was characterized by weak to moderate upwelling, strong stratification inside the bay, and higher temperatures. These conditions have been shown to be particularly favorable for large dinoflagellate blooms, which tend to outcompete diatoms in nutrient-limited and strongly stratified waters, and as such upwelling bays have described as local bloom incubators (Ryan et al., 2008; Silva et al., 2009; Barth et al., 2020). The subsequent decomposition of these localized nearshore blooms, coupled with high retention and strong stratification that acts as a barrier to vertical mixing of more oxygenated surface waters to the bottom layer, likely led to localized hypoxic conditions inside the bay (e.g., Fig. 9, Cluster 3). Similar findings were documented in a retentive bay system located along the Benguela Current (St. Helena Bay, South Africa), where locally-enhanced DO depletion followed the decay of high biomass dinoflagellate blooms and vertical fluxes of organic matter to the benthic environment (Bailey, 1991; Pitcher and Probyn, 2011; Pitcher et al., 2014, 2022). Thus, this second regime can be characterized as a coupled nearshore physical-biological process whereby strong stratification decouples surface and bottom waters, thereby enhancing the local respiration-driven drawdown inside the bay in the benthic layer.

Previous studies investigating inner shelf and nearshore DO dynamics in the California Current, largely from studies on the Oregon and Washington shelves, have documented a confluence of physical and biological processes modulating seasonal changes in DO on the shelf scale (Grantham et al., 2004; Connolly et al., 2010; Adams et al., 2013, 2016; Siedlecki et al., 2015). In these studies, the interplay between shelf-scale physical and biological processes was examined, with a conceptual model emerging of wind-driven coastal upwelling initiating the advection of low DO waters across the shelf followed by a combination of biogeochemical processes in both the water column and sediment leading to a further consumption of DO throughout the spring

and summer which was often buffered by the advection of along-shelf and cross-shelf DO gradients and/or diffusive fluxes on the shelf (see e.g., Connolly et al., 2010; Adams et al., 2013; Siedlecki et al., 2015). Here, we show that similarly coupled physical-biological processes inside the bay in the nearshore can further modify DO variability and the regional shelf-scale DO signal on a highly localized scale. Utilizing a regional collaborative network of nearshore DO measurements ranging from Central and Southern California to Baja California, Mexico, Low et al. (2021) also documented evidence of regional-scale influences of upwelling on DO dynamics across the network coupled with respiration-driven hypoxia at smaller spatial scales in the nearshore at select sites in Baja California, the latter of which was inferred from decreases in correlations between nearshore temperature and DO that occurred in the late summer and fall. We documented a similar seasonal transition inside the bay (MB and SB) between upwelling-driven hypoxia in the spring and local respiration-driven hypoxia (mediated by strong stratification and dinoflagellate blooms) later in the summer. However, outside the bay (NB), the T-DO patterns and lack of a late summer respiration-driven hypoxic regime were more similar to the geographically-similar California sites in Low et al. (2021), suggesting that upwelling bays can act as nearshore hotspots for hypoxia risk. The absence of the second hypoxic regime outside the bay was likely driven by some combination of the lack of stratification, smaller residence times, and possibly the lack of localized blooms and/or fluxes or organic matter to the benthic environment.

Further elucidation of the biological processes that contribute to nearshore DO dynamics is needed. Since decreased DO due to respiration is coupled with increasing CO_2, the impact of pH on microbial activity is important to consider (Das and Mangwani, 2015; Bunse et al., 2016). While bacterial responses to increasing CO_2 have varied across studies in different regions, several studies indicate that bacterial production and extracellular enzyme activity will increase with increasing CO_2 (Grossart et al., 2006; Piontek et al., 2010). However, elevated bacterial respiration has been shown to accompany this increase in bacterial abundance and production, suggesting a reduced growth efficiency of bacteria under high CO_2. (Fuentes-Lema et al., 2018). Temperature has been shown to influence microbial growth rate and efficiency; however, the net impact of temperature appears to be dependent on both resource availability and predation pressure (Arandia-Gorostidi et al., 2017; Morán et al., 2018). Furthermore, seasonal differences in microbial communities responsible for organic matter degradation might also drive changes in respiration rates (Ward et al., 2017; Reji et al., 2020; Nguyen et al., 2022). Finally, variability in the phytoplankton composition, particularly associated with the late summer to early fall regional upwelling relaxation season, will be important to consider. The ability of some dinoflagellate species to exhibit vertical migration (Ryan et al., 2010) and others to form resting stages (e.g., cysts; Brosnahan et al., 2020) will also lead to variations in DO dynamics. Variations in DO will potentially contribute to variations in dinoflagellate composition since DO concentrations (and temperature) can influence the formation of cysts and the germination back to vegetative states (Ellegaard and Ribeiro, 2018; Brosnahan et al., 2020). An exploration of net community production, respiration, and benthic-pelagic coupling (e.g., Pitcher et al., 2022) in the context of the physical variability is needed to understand the collective impact of these biological processes on DO dynamics in SLO Bay and other upwelling bay systems.

4.2. Upwelling bays as "Canaries on the Coast"

In both near-bottom nearshore hypoxic regimes identified, there was a clear seasonal progression and delineation of the role that physical processes play in mediating and enhancing other biotic processes that shape the local DO signal. In the first regime, strong upwelling caused the cross-shelf advection of low DO, respiration-dominated subthermocline waters on the shelf into the nearshore. In the second regime, strong vertical stratification decoupled surface and bottom waters, which likely acted to enhance local respiration-driven drawdown inside the bay. The seasonal transition between the two regimes is linked with strong seasonality in upwelling wind forcing (e.g., García-Reyes and Largier, 2012; Walter et al., 2018) and concomitant changes to both the water column stability and phytoplankton community composition (e.g., Barth et al., 2020). We highlight that nearshore hypoxia risk is highly variable over short spatial scales (on the order of km) due to the presence of a small coastal embayment. While regional-scale coastal upwelling is a first-order control on nearshore DO dynamics through its influence on productivity, stratification, and mixing, spatially variable and localized biotic and abiotic processes in the nearshore can enhance DO variability and local hypoxia risk in and around upwelling bays.

The presence of nearshore marine microclimates has been studied extensively for their ability to provide natural refuge from larger-scale climatic and regional-scale variability (e.g., Woodson et al., 2019). However, coastal embayments may act to increase ecosystem vulnerability due to their propensity for local-scale modification of both physical and biological processes. Coastal embayments reduce wind-driven upwelling (so-called upwelling shadows), leading to anomalously high surface temperatures, stratified conditions, and long residence times relative to the open coastline, all of which contribute to the formation of local bloom incubators, including many HABs species (Graham and Largier, 1997; Walter et al., 2018; Largier, 2020). The subsequent decomposition of these localized blooms, coupled with strong stratification and high retention, can drive highly localized hypoxic (and low pH) conditions. Moreover, the localized low DO events observed inside the bay during the respiration-driven hypoxic regime (Fig. 9 and Table 1, Cluster 3) are at higher temperatures compared to the upwelling-driven hypoxic regime (Fig. 9 and Table 1, Cluster 1), which could exacerbate the severity of these low DO events to organisms in the bay since survival times of marine benthic organisms under hypoxia have been shown to decrease and lethal concentrations increase at higher temperatures (Vaquer-Sunyer and Duarte, 2011). Thus, upwelling bays are likely to be at the forefront of ecosystem impacts of climate change and may act as sentinel systems or "canaries on the coast," representing an urgent need to better understand these ubiquitous features found globally in EBUS (see e.g., Table 1 in Largier, 2020, which provides a partial list of upwelling bays in EBUS). Their role as sentinels is due to their critical role for a host of processes including potential marine heatwave exposure; hypoxia development and coastal acidification (Pitcher et al., 2014); larval retention, dispersal, and connectivity (Largier, 2020); local productivity and the development of harmful algal blooms (Ryan et al., 2008; Barth et al., 2020); and nearshore circulation patterns, including exchange with the broader coastal system (Roughan et al., 2005; Trautman and Walter, 2021).

Further observations will be required to understand the longer-term persistence of the patterns detailed here, given the significant interannual variability and climate patterns detailed in the broader California Current System (Di Lorenzo et al., 2008, 2013; Macias et al., 2012). In SLO Bay, the state of both the Pacific Decadal Oscillation (PDO) and North Pacific Gyre Oscillation (NPGO), exert a strong control on the seasonality of phytoplankton community succession and the transition between diatom- and dinoflagellate-dominated periods (Barth et al., 2020; see also Fischer et al., 2020 from Monterey Bay). For example, during negative PDO years there was largely an absence of a fall dinoflagellate-dominated period, while during positive PDO years the shift to a fall dinoflagellate-dominated community occurred earlier in the seasonal cycle (Barth et al., 2020). The positive PDO is characterized by warmer surface temperatures and increased stratification, both of which are expected to increase under climate-change-driven ocean warming (Di Lorenzo et al., 2008; Li et al., 2020). Thus, continued ocean warming could provide conditions favorable for an increase in locally-enhanced respiration-driven hypoxia in nearshore embayments following the decay of dinoflagellate blooms. Moreover, further intensification of upwelling wind forcing in EBUS may lead to additional

changes to nearshore productivity and water column stability, the detailed effects of which are uncertain but potentially impactful for nearshore DO dynamics (Bakun, 1990; Sydeman et al., 2014; Wang et al., 2015; Xiu et al., 2018). As hypoxia emerges as an increasingly important climate change stressor in nearshore systems, even relative to the broader shelf (cf. Booth et al., 2014), a further understanding of drivers and ecosystem vulnerabilities is needed through sustained long-term monitoring. This study demonstrates a multiple-driver spatial mosaic of nearshore DO dynamics and highlights the need for assessing hypoxia risk and ecosystem vulnerabilities at smaller spatial scales than typically considered.

CRediT authorship contribution statement

Ryan K. Walter: Writing – review & editing, Writing – original draft, Visualization, Supervision, Software, Resources, Project administration, Methodology, Investigation, Funding acquisition, Formal analysis, Conceptualization. **Stephen A. Huie:** Writing – review & editing, Writing – original draft, Software, Formal analysis. **Jon Christian P. Abraham:** Writing – review & editing, Software, Formal analysis. **Alexis Pasulka:** Writing – review & editing, Conceptualization. **Kristen A. Davis:** Writing – review & editing, Resources, Conceptualization. **Thomas P. Connolly:** Writing – review & editing, Conceptualization. **Piero L.F. Mazzini:** Writing – review & editing, Conceptualization. **Ian Robbins:** Writing – review & editing, Conceptualization.

Declaration of competing interest

The authors declare that they have no known competing financial interests or personal relationships that could have appeared to influence the work reported in this paper.

Data availability

Data will be made available on request.

Acknowledgements

This work was supported by California Sea Grant (Award NA14OAR417007). We acknowledge support from the NOAA IOOS program through CeNCOOS (Shore Stations) and SCCOOS (HABs) for data collected at the Cal Poly Pier. We also acknowledge support from The William and Linda Frost Fund at Cal Poly. We thank Jason Felton, Tom Moylan, Emma Reid, Edwin Rainville, Tatjana Ellis, and Grant Waltz for help in the field. Boating resources were provided by the Cal Poly Center for Coastal Marine Sciences. Comments and suggestions from two anonymous reviewers improved this manuscript.

Appendix A. Supplementary data

Supplementary data to this article can be found online at https://doi.org/10.1016/j.ecss.2022.108123.

References

Adams, K.A., Barth, J.A., Chan, F., 2013. Temporal variability of near-bottom dissolved oxygen during upwelling off central Oregon. J. Geophys. Res. Ocean. 118, 4839–4854. https://doi.org/10.1002/jgrc.20361.

Adams, K.A., Barth, J.A., Shearman, R.K., 2016. Intraseasonal cross-shelf variability of hypoxia along the Newport, Oregon, hydrographic line. J. Phys. Oceanogr. 46, 2219–2238. https://doi.org/10.1175/JPO-D-15-0119.1.

Anderson, C.R., Siegel, D.A., Brzezinski, M.A., Guillocheau, N., 2008. Controls on temporal patterns in phytoplankton community structure in the Santa Barbara Channel, California. J. Geophys. Res. Ocean. 113 https://doi.org/10.1029/2007JC004321.

Arandia-Gorostidi, N., Huete-Stauffer, T.M., Alonso-Sáez, L., G.Morán, X.A., 2017. Testing the metabolic theory of ecology with marine bacteria: different temperature sensitivity of major phylogenetic groups during the spring phytoplankton bloom. Environ. Microbiol. 19, 4493–4505. https://doi.org/10.1111/1462-2920.13898.

Bailey, G.W., 1991. Organic carbon flux and development of oxygen deficiency on the modern Benguela continential shelf south of 22°S: spatial and temporal variability. Geol. Soc. London, Spec. Publ. 58, 171. https://doi.org/10.1144/GSL.SP.1991.058.01.12. LP – 183.

Bakun, A., 1990. Global climate change and intensification of coastal ocean upwelling. Science 247 (4939), 198–201. https://doi.org/10.1126/science.247.4939.198.

Barth, A., Walter, R.K., Robbins, I., Pasulka, A., 2020. Seasonal and interannual variability of phytoplankton abundance and community composition on the Central Coast of California. Mar. Ecol. Prog. Ser. 637, 29–43. https://doi.org/10.3354/meps13245.

Booth, J.A.T., McPhee-Shaw, E.E., Chua, P., Kingsley, E., Denny, M., Phillips, R., Bograd, S.J., Zeidberg, L.D., Gilly, W.F., 2012. Natural intrusions of hypoxic, low pH water into nearshore marine environments on the California coast. Continent. Shelf Res. 45, 108–115. https://doi.org/10.1016/j.csr.2012.06.009.

Booth, J.A.T., Woodson, C.B., Sutula, M., Micheli, F., Weisberg, S.B., Bograd, S.J., Steele, A., Schoen, J., Crowder, L.B., 2014. Patterns and potential drivers of declining oxygen content along the southern California coast. Limnol. Oceanogr. 59, 1127–1138. https://doi.org/10.4319/lo.2014.59.4.1127.

Breitburg, D., et al., 2018. Declining oxygen in the global ocean and coastal waters. Science 359 (80-), eaam7240. https://doi.org/10.1126/science.aam7240.

Brosnahan, M.L., Fischer, A.D., Lopez, C.B., Moore, S.K., Anderson, D.M., 2020. Cyst-forming dinoflagellates in a warming climate. Harmful Algae 91, 101728. https://doi.org/10.1016/j.hal.2019.101728.

Bunse, C., Lundin, D., Karlsson, C.M.G., Akram, N., Vila-Costa, M., Palovaara, J., Svensson, L., Holmfeldt, K., González, J.M., Calvo, E., Pelejero, C., Marrasé, C., Dopson, M., Gasol, J.M., Pinhassi, J., 2016. Response of marine bacterioplankton pH homeostasis gene expression to elevated CO2. Nat. Clim. Change 6, 483–487. https://doi.org/10.1038/nclimate2914.

Chan, F., Barth, J.A., Lubchencho, J., Kirincich, A., Weeks, H., Peterson, W.T., Menge, B. A., 2008. Emergence of anoxia in the California current large marine ecosystem. Science 319 (80-), 920. https://doi.org/10.1126/science.1149016.

Chavez, F.P., Messié, M., 2009. A comparison of eastern boundary upwelling ecosystems. Prog. Oceanogr. 83, 80–96. https://doi.org/10.1016/j.pocean.2009.07.032.

Checkley, D.M., Barth, J.A., 2009. Patterns and processes in the California current system. Prog. Oceanogr. 83, 49–64. https://doi.org/10.1016/j.pocean.2009.07.028.

Connolly, T.P., Hickey, B.M., Geier, S.L., Cochlan, W.P., 2010. Processes influencing seasonal hypoxia in the northern California Current System. J. Geophys. Res. Ocean. 115 https://doi.org/10.1029/2009JC005283.

Das, S., Mangwani, N., 2015. Ocean acidification and marine microorganisms: responses and consequences. Oceanologia 57, 349–361. https://doi.org/10.1016/j.oceano.2015.07.003.

Di Lorenzo, E., Combes, V., Keister, J.E., Strub, P.T., Thomas, A.C., Franks, P.J.S., Ohman, M.D., Furtado, J.C., Bracco, A., Bograd, S.J., Peterson, W.T., Schwing, F.B., Chiba, S., Taguchi, B., Hormazabal, S., Parada, C., 2013. Synthesis of pacific ocean climate and ecosystem dynamics. Oceanography 26, 68–81. https://doi.org/10.5670/oceanog.2013.76.

Di Lorenzo, E., Schneider, N., Cobb, K.M., Franks, P.J.S., Chhak, K., Miller, A.J., McWilliams, J.C., Bograd, S.J., Arango, H., Curchitser, E., Powell, T.M., Rivière, P., 2008. North Pacific Gyre Oscillation links ocean climate and ecosystem change. Geophys. Res. Lett. 35 https://doi.org/10.1029/2007GL032838.

Ekau, W., Auel, H., Portner, H.O., Gilbert, D., 2010. Impacts of hypoxia on the structure and processes in pelagic communities (zooplankton, macro-invertebrates and fish). Biogeosciences 7, 1669–1699. https://doi.org/10.5194/bg-7-1669-2010.

Ellegaard, M., Ribeiro, S., 2018. The long-term persistence of phytoplankton resting stages in aquatic 'seed banks'. Biol. Rev. 93, 166–183. https://doi.org/10.1111/brv.12338.

Emery, W.J., Thomson, R.E., 2004. Data Analysis Methods in Physical Oceanography, second ed. Elsevier, Amsterdam, p. 638.

Fischer, A.D., Hayashi, K., McGaraghan, A., Kudela, R.M., 2020. Return of the "age of dinoflagellates" in Monterey Bay: drivers of dinoflagellate dominance examined using automated imaging flow cytometry and long-term time series analysis. Limnol. Oceanogr. 65, 2125–2141. https://doi.org/10.1002/lno.11443.

Frieder, C.A., Nam, S.H., Martz, T.R., Levin, L.A., Division, O., Science, A., Diego, S., 2012. High temporal and spatial variability of dissolved oxygen and pH in a nearshore California kelp forest. Biogeosciences 3917–3930. https://doi.org/10.5194/bg-9-3917-2012.

Fuentes-Lema, A., Sanleón-Bartolomé, H., Lubián, L.M., Sobrino, C., 2018. Effects of elevated CO2 and phytoplankton-derived organic matter on the metabolism of bacterial communities from coastal waters. Biogeosciences 15, 6927–6940. https://doi.org/10.5194/bg-15-6927-2018.

García-Reyes, M., Largier, J.L., 2012. Seasonality of coastal upwelling off central and northern California: New insights, including temporal and spatial variability. J. Geophys. Res. Oceans 117 (C3). https://doi.org/10.1029/2011JC007629.

Gilbert, D., Rabalais, N.N., Díaz, R.J., Zhang, J., 2010. Evidence for greater oxygen decline rates in the coastal ocean than in the open ocean. Biogeosciences 7, 2283–2296. https://doi.org/10.5194/bg-7-2283-2010.

Graham, W.M., Largier, J.L., 1997. Upwelling shadows as nearshore retention sites: the example of northern Monterey Bay. Continent. Shelf Res. 17, 509–532. https://doi.org/10.1016/S0278-4343(96)00045-3.

Grantham, B.A., Chan, F., Nielsen, K.J., Fox, D.S., Barth, J.A., Huyer, A., Lubchenco, J., Menge, B.A., 2004. Upwelling-driven nearshore hypoxia signals ecosystem and oceanographic changes in the northeast Pacific. Nature 429, 749–754. https://doi.org/10.1038/nature02605.

Gray, J.S., Wu, R.S., Or, Y.Y., 2002. Effects of hypoxia and organic enrichment on the coastal marine environment. Mar. Ecol. Prog. Ser. 238, 249–279. https://www.int-res.com/abstracts/meps/v238/p249-279/.

Grossart, H.-P., Allgaier, M., Passow, U., Riebesell, U., 2006. Testing the effect of CO2 concentration on the dynamics of marine heterotrophic bacterioplankton. Limnol. Oceanogr. 51, 1–11. https://doi.org/10.4319/lo.2006.51.1.0001.

Guadayol, O., Silbiger, N.J., Donahue, M.J., Thomas, F.I.M., 2014. Patterns in temporal variability of temperature, oxygen and pH along an environmental gradient in a coral reef. PLoS One 9, e85213.

Hofmann, A.F., Peltzer, E.T., Waltz, P.M., Brewer, P.G., 2011. Hypoxia by degrees: Establishing definitions for a changing ocean. Deep Sea Res. Part I 58 (12), 1212–1226. https://doi.org/10.1016/j.dsr.2011.09.004.

Horner-Devine, A.R., Hetland, R.D., MacDonald, D.G., 2015. Mixing and transport in coastal river plumes. Annu. Rev. Fluid Mech. 47, 569–594. https://doi.org/10.1146/annurev-fluid-010313-141408.

Kapsenberg, L., Cyronak, T., 2019. Ocean acidification refugia in variable environments. Global Change Biol. 25, 3201–3214. https://doi.org/10.1111/gcb.14730.

Keeling, R.E., Körtzinger, A., Gruber, N., 2010. Ocean deoxygenation in a warming world. Ann. Rev. Mar. Sci 2, 199–229. https://doi.org/10.1146/annurev.marine.010908.163855.

Kessouri, F., McWilliams, J.C., Bianchi, D., Sutula, M., Renault, L., Deutsch, C., Feely, R. A., McLaughlin, K., Ho, M., Howard, E.M., Bednaršek, N., Damien, P., Molemaker, J., Weisberg, S.B., 2021. Coastal eutrophication drives acidification, oxygen loss, and ecosystem change in a major oceanic upwelling system. Proc. Natl. Acad. Sci. USA 118 (21), e2018856118. https://doi.org/10.1073/pnas.2018856118.

Lance, G.N., Williams, W.T., 1967. A general theory of classificatory sorting strategies: II. Clustering systems. Comput. J. 10, 271–277. https://doi.org/10.1093/comjnl/10.3.271.

Largier, J.L., 2020. Upwelling bays: how coastal upwelling controls circulation, habitat, and productivity in bays. Ann. Rev. Mar. Sci 12, 415–447. https://doi.org/10.1146/annurev-marine-010419-011020.

Leary, P.R., Woodson, C.B., Squibb, M.E., Denny, M.W., Monismith, S.G., Micheli, F., 2017. Internal tide pools" prolong kelp forest hypoxic events. Limnol. Oceanogr. 62, 2864–2878. https://doi.org/10.1002/lno.10716.

Lentz, S.J., Fewings, M.R., 2011. The wind- and wave-driven inner-shelf circulation. Ann. Rev. Mar. Sci 4, 317–343. https://doi.org/10.1146/annurev-marine-120709-142745.

Li, G., Cheng, L., Zhu, J., Trenberth, K.E., Mann, M.E., Abraham, J.P., 2020. Increasing ocean stratification over the past half-century. Nat. Clim. Change 10, 1116–1123. https://doi.org/10.1038/s41558-020-00918-2.

Low, N.H.N., Micheli, F., Aguilar, J.D., Arce, D.R., Boch, C.A., Bonilla, J.C., Bracamontes, M.Á., De Leo, G., Diaz, E., Enríquez, E., Hernandez, A., Martinez, R., Mendoza, R., Miranda, C., Monismith, S., Ramade, M., Rogers-Bennett, L., Romero, A., Salinas, C., Smith, A.E., Torre, J., Villavicencio, G., Woodson, C.B., 2021. Variable coastal hypoxia exposure and drivers across the southern California Current. Sci. Rep. 11, 10929 https://doi.org/10.1038/s41598-021-89928-4.

Macias, D., Landry, M.R., Gershunov, A., Miller, A.J., Franks, P.J.S., 2012. Climatic control of upwelling variability along the Western north-American coast. PLoS One 7, e30436.

Mattiasen, E.G., Kashef, N.S., Stafford, D.M., Logan, C.A., Sogard, S.M., Bjorkstedt, E.P., Hamilton, S.L., 2020. Effects of hypoxia on the behavior and physiology of kelp forest fishes. Global Change Biol. 26 (6), 3498–3511. https://doi.org/10.1111/gcb.15076.

McSweeney, J.M., Lerczak, J.A., Barth, J.A., Becherer, J., MacKinnon, J.A., Waterhouse, A.F., Colosi, J.A., MacMahan, J.H., Feddersen, F., Calantoni, J., Simpson, A., Celona, S., Haller, M.C., Terrill, E., 2020. Alongshore variability of shoaling internal bores on the inner shelf. J. Phys. Oceanogr. 50, 2965–2981. https://doi.org/10.1175/JPO-D-20-0090.1.

Morán, X.A.G., Calvo-Díaz, A., Arandia-Gorostidi, N., Huete-Stauffer, T.M., 2018. Temperature sensitivities of microbial plankton net growth rates are seasonally coherent and linked to nutrient availability. Environ. Microbiol. 20, 3798–3810. https://doi.org/10.1111/1462-2920.14393.

Nguyen, V., Anderson, P., Pasulka, A., Migler, T., 2022. Analysis of the San Luis Obispo Bay Microbiome from a Network Perspective BT - Complex Networks & Their Applications X. Springer Nature Switzerland AG, pp. 664–675.

Nickols, K.J., Gaylord, B., Largier, J.L., 2012. The coastal boundary layer: predictable current structure decreases alongshore transport and alters scales of dispersal. Mar. Ecol. Prog. Ser. 464, 17–35. https://doi.org/10.3354/meps09875.

Piontek, J., Lunau, M., Händel, N., Borchard, C., Wurst, M., Engel, A., 2010. Acidification increases microbial polysaccharide degradation in the ocean. Biogeosciences 7, 1615–1624. https://doi.org/10.5194/bg-7-1615-2010.

Pitcher, G.C., Probyn, T.A., 2011. Anoxia in southern Benguela during the autumn of 2009 and its linkage to a bloom of the dinoflagellate *Ceratium balechii*. Harmful Algae 11, 23–32.

Pitcher, G.C., Probyn, T.A., du Randt, A., 2022. Changes in water column oxygen, estimates of productivity and the development of anoxia in a major embayment of the southern Benguela eastern boundary upwelling system. J. Mar. Syst. 227, 103694 https://doi.org/10.1016/j.jmarsys.2021.103694.

Pitcher, G.C., Probyn, T.A., du Randt, A., Lucas, A.J., Bernard, S., Evers-King, H., Lamont, T., Hutchings, L., 2014. Dynamics of oxygen depletion in the nearshore of a coastal embayment of the southern Benguela upwelling system. J. Geophys. Res. Ocean. 119, 2183–2200. https://doi.org/10.1002/2013JC009443.

Reji, L., Tolar, B.B., Chavez, F.P., Francis, C.A., 2020. Depth-differentiation and seasonality of planktonic microbial assemblages in the Monterey bay upwelling system. Front. Microbiol. 11, 1075. https://doi.org/10.3389/fmicb.2020.01075.

Roughan, M., Mace, A.J., Largier, J.L., Morgan, S.G., Fisher, J.L., Carter, M.L., 2005. Subsurface recirculation and larval retention in the lee of a small headland: a variation on the upwelling shadow theme. J. Geophys. Res. Ocean. 110 https://doi.org/10.1029/2005JC002898.

Ryan, J.P., Gower, J.F.R., King, S.A., Bissett, W.P., Fischer, A.M., Kudela, R.M., Kolber, Z., Mazzillo, F., Rienecker, E.V., Chavez, F.P., 2008. A coastal ocean extreme bloom incubator. Geophys. Res. Lett. 35 https://doi.org/10.1029/2008GL034081.

Ryan, J.P., McManus, M.A., Sullivan, J.M., 2010. Interacting physical, chemical and biological forcing of phytoplankton thin-layer variability in Monterey Bay, California. Continent. Shelf Res. 30, 7–16. https://doi.org/10.1016/j.csr.2009.10.017.

Siedlecki, S.A., Banas, N.S., Davis, K.A., Giddings, S., Hickey, B.M., MacCready, P., Connolly, T., Geier, S., 2015. Seasonal and interannual oxygen variability on the Washington and Oregon continental shelves. J. Geophys. Res. Ocean. 120, 608–633. https://doi.org/10.1002/2014JC010254.

Silva, A., Palma, S., Oliveira, P.B., Moita, M.T., 2009. Composition and interannual variability of phytoplankton in a coastal upwelling region (Lisbon Bay, Portugal). J. Sea Res. 62, 238–249. https://doi.org/10.1016/j.seares.2009.05.001.

Sinnett, G., Feddersen, F., Lucas, A.J., Pawlak, G., Terrill, E., 2018. Observations of nonlinear internal wave run-up to the surfzone. J. Phys. Oceanogr. 48, 531–554. https://doi.org/10.1175/JPO-D-17-0210.1.

Sydeman, W.J., Garcia-Reyes, M., Schoeman, D.S., Rykaczewski, R.R., Thompson, S.A., Black, B.A., Bograd, S.J., 2014. Climate change and wind intensification in coastal upwelling ecosystems. Science 345 (80-), 77–80. https://doi.org/10.1126/science.1251635.

Trautman, N., Walter, R.K., 2021. Seasonal variability of upwelling and downwelling surface current patterns in a small coastal embayment. Continent. Shelf Res. 226, 104490 https://doi.org/10.1016/j.csr.2021.104490.

Valera, M., Walter, R.K., Bailey, B.A., Castillo, J.E., 2020. Machine learning based predictions of dissolved oxygen in a small coastal embayment. J. Mar. Sci. Eng. https://doi.org/10.3390/jmse8121007.

Vaquer-Sunyer, R., Duarte, C.M., 2008. Thresholds of hypoxia for marine biodiversity. Global Change Biol. 17 (5), 1788–1797. https://doi.org/10.1111/j.1365-2486.2010.02343.x.

Vaquer-Sunyer, R., Duarte, C.M., 2011. Temperature effects on oxygen thresholds for hypoxia in marine benthic organisms. Proc. Natl. Acad. Sci. USA 105 (40), 15452–15457. https://doi.org/10.1073/pnas.0803833105.

Walter, R.K., Armenta, K.J., Shearer, B., Robbins, I., Steinbeck, J., 2018. Coastal upwelling seasonality and variability of temperature and chlorophyll in a small coastal embayment. Continent. Shelf Res. 154, 9–18. https://doi.org/10.1016/j.csr.2018.01.002.

Walter, R.K., Reid, E.C., Davis, K.A., Armenta, K.J., Merhoff, K., Nidzieko, N.J., 2017. Local diurnal wind-driven variability and upwelling in a small coastal embayment. J. Geophys. Res. Ocean. 122, 955–972. https://doi.org/10.1002/2016JC012466.

Walter, R.K., Squibb, M.E., Woodson, C.B., Koseff, J.R., Monismith, S.G., 2014b. Stratified turbulence in the nearshore coastal ocean: dynamics and evolution in the presence of internal bores. J. Geophys. Res. Ocean. 119, 8709–8730. https://doi.org/10.1002/2014JC010396.

Walter, R.K., Woodson, C.B., Arthur, R.S., Fringer, O.B., Monismith, S.G., 2012. Nearshore internal bores and turbulent mixing in southern Monterey Bay. J. Geophys. Res. Ocean. 117 https://doi.org/10.1029/2012JC008115.

Walter, R.K., Woodson, C.B., Leary, P.R., Monismith, S.G., 2014a. Connecting wind-driven upwelling and offshore stratification to nearshore internal bores and oxygen variability. J. Geophys. Res. Ocean. 119, 3517–3534. https://doi.org/10.1002/2014JC009998.

Wang, D., Gouhier, T.C., Menge, B.A., Ganguly, A.R., 2015. Intensification and spatial homogenization of coastal upwelling under climate change. Nature 518, 390–394. https://doi.org/10.1038/nature14235.

Wang, Y., Walter, R.K., White, C., Ruttenberg, B.I., 2022. Spatial and temporal characteristics of California commercial fisheries from 2005 to 2019 and potential overlap with offshore wind energy development. Marine and Coastal Fisheries 14 (4), e10215. https://doi.org/10.1002/mcf2.10215.

Ward, C.S., Yung, C.-M., Davis, K.M., Blinebry, S.K., Williams, T.C., Johnson, Z.I., Hunt, D.E., 2017. Annual community patterns are driven by seasonal switching between closely related marine bacteria. ISME J. 11, 1412–1422. https://doi.org/10.1038/ismej.2017.4.

Woodson, C.B., 2013. Spatiotemporal variation in cross-shelf exchange across the inner shelf of Monterey bay, California. J. Phys. Oceanogr. 43, 1648–1665. https://doi.org/10.1175/JPO-D-11-0185.1.

Woodson, C.B., Eerkes-Medrano, D.I., Flores-Morales, A., Foley, M.M., Henkel, S.K., Hessing-Lewis, M., Jacinto, D., Needles, L., Nishizaki, M.T., O'Leary, J., Ostrander, C.E., Pespeni, M., Schwager, K.B., Tyburczy, J.A., Weersing, K.A., Kirincich, A.R., Barth, J.A., McManus, M.A., Washburn, L., 2007. Local diurnal upwelling driven by sea breezes in northern Monterey Bay. Continent. Shelf Res. 27, 2289–2302. https://doi.org/10.1016/j.csr.2007.05.014.

Woodson, C.B., Micheli, F., Boch, C., Al-Najjar, M., Espinoza, A., Hernandez, A., Vázquez-Vera, L., Saenz-Arroyo, A., Monismith, S.G., Torre, J., 2019. Harnessing marine microclimates for climate change adaptation and marine conservation. Conserv. Lett. 12, 1–9. https://doi.org/10.1111/conl.12609.

Xiu, P., Chai, F., Curchitser, E.N., Castruccio, F.S., 2018. Future changes in coastal upwelling ecosystems with global warming: the case of the California Current System. Sci. Rep. 8, 2866. https://doi.org/10.1038/s41598-018-21247-7.